Supermodes in Broad Ridge (Al,In)GaN Laser Diodes

Harald Braun, Stephan Rogowsky, Ulrich T. Schwarz, Stefanie Brüninghoff, Alfred Lell, Stephan Lutgen, and Uwe Strauß

***Abstract*—Broad area (Al,In)GaN laser diodes (LDs) are suitable for high optical output power in the near UV to blue spectral range. But for ridge widths larger than a few micrometers, the occurrence of filamentation is well known. We present experimental evidence that the single filaments tend to be phase-locked with defined phase offset and build up a so called supermode. Depending on driving current a coherent or incoherent superposition of different supermodes can be observed, which has a significant impact on the corresponding lateral far-field pattern. By a simulated reconstruction of the lateral mode profile of the laser mode propagating in free space we retrieve the field and phase distribution of the laser mode in the waveguide. In this context the coupling mechanism is discussed and the mode behavior is compared to supermodes in GaAs laser diode arrays.**

***Index Terms*—Gallium compounds, laser modes, semiconductor lasers.**

I. Introduction

BLUE or near UV (Al,In)GaN laser diodes (LDs) with optical output power of around 100 mW are commercially available and are, concerning lifetime and beam quality, suitable for applications like high density optical data storage or pico-size projection [1]. But optical output power and beam quality have to be improved for further demanding applications like large scale laser projection. When output power of a LD shall be further increased, the optical power density in the waveguide is the limiting factor. If the optical power density at the facet of the LD exceeds a certain level, catastrophic optical mirror damage (COMD) occurs. Thus the cross section area of the optical mode has to be increased.

One possibility is extending the mode volume in transversal direction by an enlargements of the epitaxial waveguide layer thickness [2]. But the gain region consisting of InGaN quantum wells (QWs) cannot be stretched in the same way, because the number of QWs is limited due to piezoelectric effects and the high hole mass in the (Al,In)GaN system. Hence an enlargement of the waveguide thickness leads consequentially to a lower confinement factor and thus to an increasing threshold current.

Manuscript received December 22, 2008; revised March 11, 2009. Current version published July 29, 2009.

H. Braun, S. Rogowsky, and U. T. Schwarz are with the Institut für Angewandte und Experimentelle Physik, University of Regensburg, 93053 Regensburg, Germany (e-mail: harald.braun@physik.uni-regensburg.de; stephan.rogowsky@physik.uni-regensburg.de; uli.schwarz@physik.uni-regensburg.de).

S. Brüninghoff, A. Lell, S. Lutgen, and U. Strauß are with Osram Opto Semiconductors GmbH, 93055 Regensburg, Germany (e-mail: stefanie.brueninghoff@osram-os.com; alfred.lell@osram-os.com; stephan.lutgen@osram-os.com; uwe.strauss@osram-os.com).

Digital Object Identifier 10.1109/JQE.2009.2019614

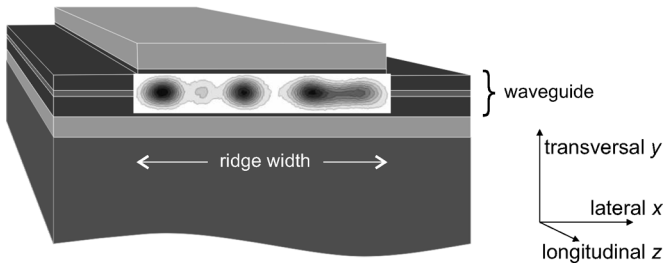

Fig. 1. Sketch of a broad ridge (Al,In)GaN LD. The inset shows a typical near-field measurement of the optical laser mode of a sample with a 10 μm broad ridge waveguide.

However, this deficit is acceptable to a certain degree, because in the high driving current regime slope efficiency, which is not affected by the confinement factor, is the decisive parameter to reach high output power.

The usual and more effective way to increase the mode volume is to expand the waveguide in lateral direction [2]–[5]. But lateral fundamental mode operation is limited to ridge widths of about 2 μm [6]. Due to the high antiguiding factor of (Al,In)GaN based LDs [7], a strong tendency to build up filaments is predicted for broad ridge LDs [8], [9]. Experimental evidence for filamentation in broad ridge (Al,In)GaN LDs has been shown in several publications [4], [10], [11].

Filamentation has a significant impact on the corresponding far-field pattern. In this context the spatial coherence of the laser mode plays a decisive role. In detail, filaments can be phase-locked and build up so called supermodes. Thus the far-field pattern is the result of interfering filaments. This behavior is well known in the GaAs material system [12] and will be discussed in detail for (Al,In)GaN laser diodes in this paper.

Fig. 1 shows a sketch of a broad ridge (Al,In)Gan LD. The inset of Fig. 1 shows a typical near-field measurement of the optical laser mode of a sample with a 10 μm broad ridge waveguide. There is also a slight modulation of the lateral intensity profile below threshold, but the LD is emitting much more uniformly over the whole ridge width of 10 μm. Above threshold, interplay of the photon density with the lateral refractive index profile, the local carrier density [13] and thermal effects [14] lead to self focusing of the optical laser mode, well known as filamentation [8]. In this context carrier induced changes of the local refractive index and lateral carrier diffusion in the quantum wells play an essential role. In detail, the real part of the refractive index profile of the ridge waveguide is decreased by the local carrier distribution (antiguiding) and increased following the lateral temperature profile. The local carrier density defines also the imaginary part of the refractive index, which is related to optical gain.

In [15] we presented a rate equation based model adapted to (Al,In)GaN LDs, which describes the the occurrence of filaments as incoherent superposition of perturbed higher order lateral modes, defined by the resulting modified complex refractive index profile. In this approach, no spectral information was taken into account. Now, in this article, we combine spatial and spectral information and show experimental evidence, that single filaments in broad ridge LDs are phase-locked and form so called supermodes.

The investigated samples and the experimental method are introduced in Section II. In Section III the most simple case of a single supermode is discussed in detail. We present spectral resolved near-field measurements, which indicate the existence of coupled filaments, and far-field patterns that can be explained by interference effects. The formation of this far-field pattern is illustrated by a measurement of the lateral mode profile, propagating from the near-field to the far-field. By a reconstruction of this propagation we retrieve the field and phase distribution of the optical laser mode in the waveguide. This provides essential information about the coupling mechanism. At higher driving currents we observe an incoherent superposition of different supermodes (Section IV). In this context we discuss the impact of driving current on the beam quality of broad ridge (Al,In)GaN LDs.

II. Experimental

The investigated samples are edge emitting broad ridge laser diode test structures, grown on low defect density c-plane GaN substrate by MOVPE. In this paper measurements on three samples, named A, B and C with ridge widths of 5 μm, 10 μm and 20 μm, respectively, will be shown. The corresponding threshold current densities I_{th} are 6.6 kA cm^{-2}, 1.2 kA cm^{-2} and 4.2 kA cm^{-2}, and the slope efficiencies are about 1.1 W/A, 0.8 W/A and 1.1 W/A, respectively. The emission wavelength λ is about 395 nm for samples A and C and about 445 nm for sample B. Samples A and C are optimized for high output power, which means for example that the reflectivity of the output facet is only about 17% and the thickness of the epitaxial waveguide layers is increased by 80% compared to the standard waveguide structure of sample B, which is described in detail for example in [1]. Further information about the waveguide optimization procedure regarding samples A and C can be found in [2], where optical output values of a single emitter of up to 8 W in pulsed operation are reported for similar samples. Due to these modifications samples A and C are on the one side capable for high optical output power, but on the other side their threshold current densities are quite high compared to sample B, which is completely optimized for low threshold current density but is not suitable for such high output powers. For the measurements the LDs are driven in cw mode with optical output power up to a few hundred mW, thus active cooling of the diodes is essential. While the heatsink temperature was kept constant at about 20°C, the estimated temperature of the waveguide according to measurements on similar samples [11] increases up to about 50°C under typical operating conditions used for the measurements shown in this article.

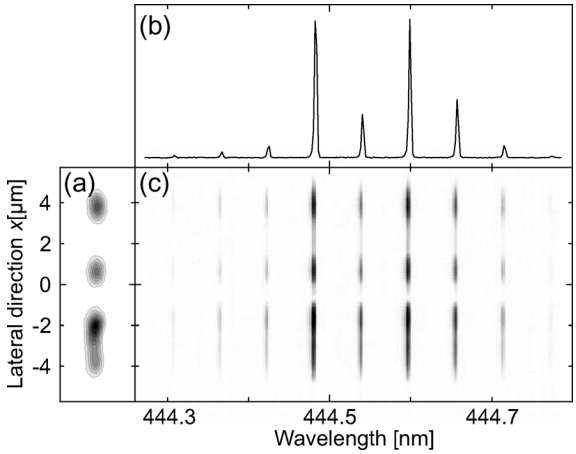

Fig. 2. (a) Near-field intensity distribution of sample B at $I = 1.23 I_{\mathrm{th}}$. (b) Spatially integrated spectrum taken under same conditions. (c) Corresponding lateral resolved spectral characterization of the lateral near-field profile.

We perform a multidimensional characterization of the optical laser mode, regarding lateral direction x, propagation direction z and wavelength λ. For this purpose we use an imaging setup in a configuration known as *Gaussian telescope*. A detailed description of this setup can be found in [16]. It consists, in principle, of a combination of two lenses L_1 and L_2 with focal lengths f_1 and f_2, respectively, arranged in a distance $f_1 + f_2$ to each other. In this way it is assured, that the transformed laser beam contains the correct phase distribution, which is essential for measurements of the propagating mode.

Due to the in transversal direction highly divergent laser beam an aspheric lens L_1 with high numeric aperture has to be used to prevent aberration artefacts. The magnification m of this configuration is simply given by the ratio of f_1/f_2.

For measurements of the near-field intensity distribution, an image of the front facet of the LD is projected onto a bare CCD-chip, located in the focal plane of the imaging setup. Alternatively a single mode fiber in combination with a high spectral resolution spectrometer was used to analyze the spectral composition of the laser mode, correlated to the spatial position. The spectral resolution of about 0.005 nm is sufficient to distinguish clearly single longitudinal modes belonging to different lateral modes. Using a magnification of $m = 35$, there is no limitation of the spatial resolution by the CCD pixel size (4.65 μm) or by the fiber diameter (3 μm).

With this setup we can as well investigate the propagation of the laser mode from the near-field to the far-field, by scanning in positive z-direction relative to the focal plane. For these measurements one has to consider that the magnification in propagation direction z is proportional to m^2. To reach the far-field within the range of some cm, accessible with the experimental setup, m has to be low enough. Alternatively the far-field intensity distribution can also be measured directly without any optical components.

III. Single Supermode

In this section we describe the formation, propagation and reconstruction of the laser mode for the case, that only one single supermode exists, which means that the laser emits coherently

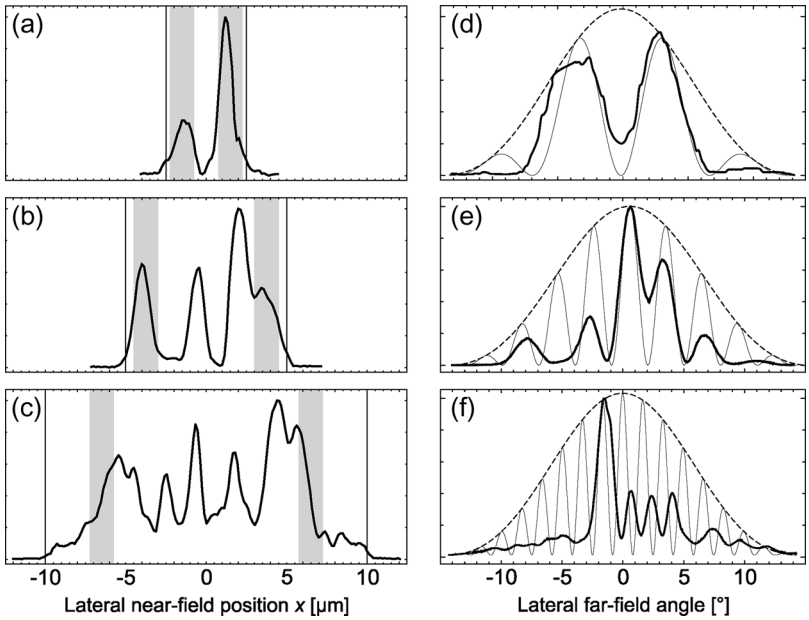

Fig. 3. (a)–(c) Lateral near-field and (d)–(f) far-field data for samples A, B and C with ridge widths of 5, 10 and 20 μm, respectively. The thick lines are experimental data. All measurements are taken at a driving current in the order of $I = 1.2I_{\rm th}$. The thin vertical lines in (a)–(c) indicate the position of the ridge waveguide, the gray bars represent the positions of the double slit used for the simulated far-field profile, shown as thin lines in (d)–(f). A single slit of 1.5 μm in the near-field would lead to the refraction pattern shown by the dashed line in (d)–(f), respectively.

over the whole ridge width. We observe such a behavior at all investigated broad ridge samples for the current regime slightly above threshold. For higher driving currents additional supermodes appear. This case will be discussed in Section IV.

A. Near-Field

The density plot in Fig. 2(a) shows the near-field intensity distribution of sample B at a driving current of about $I = 1.23I_{\rm th}$. One can clearly see a very inhomogeneous lateral mode profile. Fig. 2(b) shows the corresponding spatial integrated spectrum. It is characteristic for (Al,In)GaN LDs; several longitudinal modes are lasing. All modes have the same spectral spacing of 55 pm, which fits well to expected value for longitudinal Fabry-Perot (FP) modes of a standing wave with $\lambda = 445$ nm in the given waveguide with a length of 600 μm. Thus there exists only one single mode comb.

The spatially resolved spectral measurement, shown in Fig. 2(c) provides further information. It shows the result of a scan in lateral direction through the center of the near-field image, where a highly resolved spectrum at each point of the scan was taken. The data show, that the normalized spectrum at each point of the laser mode looks nearly identical. In other words, a replica of the near-field pattern is observed for all longitudinal modes. This indicates complete phase-locking of all filaments [12], which means that all filaments have the same effective refractive index $n_{\rm eff}$ and thus the same propagation constant.

Such an array of phase-locked filaments is also called supermode [12], [17]. It is not an usual higher order lateral mode, but self-focusing leads to the formation of filaments, and these filaments tend to be phase-locked in the same fashion as semiconductor laser arrays [17], [18]. Please note that the term "supermode" is besides used in a different context, namely for a linear combination of TE and TM lasing modes in birefringent GaInP/AlGaInP waveguides [19].

B. Far-Field

In the following details about the coupling of filaments and its impact on the corresponding far-field pattern will be discussed. The thick lines in Fig. 3 show measurements of the lateral near-field and far-field profile of the three samples A, B and C at driving currents of $I = 1.2I_{\rm th}, 1.23I_{\rm th}$ and $1.15I_{\rm th}$, respectively. All near-field measurements, depicted in Fig. 3(a)–(c), show strong filamentation, where the width of all single filaments is in the range of about 1–1.5 μm and the number of the filaments increases with increasing ridge width (compare [15]). The thin vertical lines indicate the positions of the ridge waveguide, respectively. The corresponding far-field measurements, shown in 3(d)–(f), exhibit a characteristic multi-lobed pattern. Obviously, the width of the single lobes decreases significantly with increasing ridge width, whereas the whole width of the far-field stays nearly constant.

The spectra of all three samples exhibit only one FP mode comb, respectively, under the conditions that have been used for the measurements shown in Fig. 3. As already mentioned, this indicates coupling between the filaments, and so the far-field is expected to be the result of interfering beams. To illustrate the characteristics of these interference patterns, we compare the experimental data with a virtual double-slit interference experiment, which helps to explain the general shape of the far-field spectra. Two slits with a width of $b = 1.5$ μm each represent the single filaments and the distance a between the center of the two slits is fitted to the lateral spreading of distinct coherent filaments. The gray bars in Fig. 3(a), (b) and (c) indicate the width and the position of the two slits; values of $a = 3.0$, 7.5 and 13.0 μm have been used, respectively.

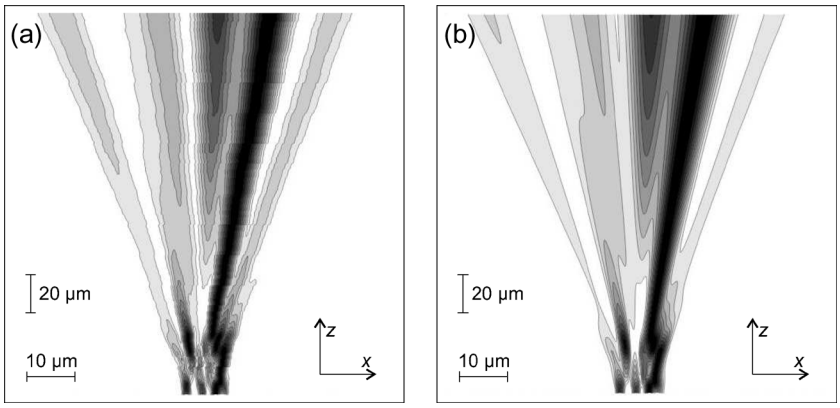

Fig. 4. (a) Experimental and (b) simulated near-field to far-field transition of the lateral intensity profile of sample B under same conditions like in Fig. 2.

The thin lines in Fig. 3(d)–(f) show the corresponding calculated interference patterns, when the double slit is illuminated with coherent light with $\lambda = 400$ nm. The lobes become narrower with increasing a, which is in good agreement with the observed behavior for increasing ridge width. The envelope of the far-field pattern, described by the dashed line in Fig. 3(d)–(f), depends only on the width b of the single slits, which represent the filaments, and is thus independent on the distance a between the slits or the ridge width, respectively.

This means on the other hand, that, if the single filaments were not coherent and would propagate independently, each filament would result in a Gaussian far-field lobe with a FWHM of about 10°. This would produce a completely different far-field pattern than it is shown in Fig. 3(d)–(f). But the filaments are coupled and this results in a multi-lobed far-field pattern. If all filaments would lock in phase, a far-field pattern with a single distinct maximum at the center would appear, like it is described in [18] for a broad ridge LD in the GaAs material system. But in all far-field measurements performed on broad ridge (Al,In)GaN laser diodes there are several intensity maxima, thus there must be a significant phase offset between the single coupled filaments. Goto *et al.* [3] show also a far-field measurement of a 10 μm broad ridge (Al,In)GaN LD, which looks quite similar to the data presented in this paper. The lateral far-field pattern is multi-lobed and the most pronounced lobe has a FWHM of about 2.3°.

C. Near-Field to Far-Field Transition

To investigate this coupling in more detail, a scan of the complete near- to far-field transition was taken. For this measurement, images of the intensity distribution in the $x - y$-plane were taken, starting from the focal point, where the image of the near-field is located, and scanning into positive z-direction. The single images are then integrated in transversal direction and normalized separately.

The measurement in Fig. 4(a) shows from bottom to top the first 200 μm of the propagation of the lateral mode profile from the near-field to the far-field of sample B at a driving current of $I = 1.23 I_{\mathrm{th}}$. One can clearly see that the lateral far-field pattern is the result of interfering filaments. But one has to note that the Rayleigh range of a LD, emitting coherently over a ridge width of 10 μm with $\lambda = 445$ nm, is larger than the range shown in Fig. 4(a). The Rayleigh range is a measure for the transition from near-field to far-field and thus this means that the far-field is not reached in this figure. During the further propagation to the far-field the central lobe at 0° becomes dominant, as it is shown in Fig. 3(e).

D. Phase Reconstruction

With a CCD camera only the intensity of the laser mode can be measured. To retrieve the field and phase distribution of the mode, the intensity distribution in at least two planes has to be measured. If the propagation function between the two planes is known, the phase distribution of the mode can be reconstructed.

For this purpose different approaches can be used. The Gerchberg-Saxton algorithm [20] for example is a common iterative procedure to determine the phase distribution from image and diffraction plane pictures. A similar method will be used in this paper. Another approach is to guess an initial phase in the near-field, calculate the near-field to far-field propagation using Fresnel diffraction integral, and then find the correct near-field phase with an optimization algorithm, using the difference between measured and calculated intensity distribution at several distances to the facet as merit function [21]. In an earlier approach to derive the phase for broad area LDs we neglected the precondition of a coherent superposition, because we had no experimental access to the spectral information [15].

Now spectrally and spatially resolved measurements presented in this paper give evidence that the laser mode of broad ridge InGaN LDs can be described as a supermode, which consists of a coherent superposition of filaments. To satisfy this physical picture of coupled filaments, we reconstruct the lateral intensity profile $\mathcal{I}(x,z)$ of the laser mode as a superposition of fields $E_j(x,z)$ of $j = (1 \ldots N)$ zeroth-order Gaussian modes, which represent the filaments.

The lateral complex electric field amplitude $E_j(x,z)$ of a Gaussian mode [22] with wave number $k = 2\pi/\lambda$ is given by

$$E_j(x,z) = A_j \exp[-i\phi_j] \frac{w_{0,j}}{w_j(z)} \exp\left[\frac{(x-\xi_j)^2}{w_j^2(z)}\right] \times \exp\left[-ikz - ik\frac{(x-\xi_j)^2}{2R_j^2(z)} + i\zeta_j(z)\right]. \quad (1)$$

Here A_j is the amplitude, ϕ_j the constant phase offset, w_j the width, ξ_j the lateral position, R_j the radius of curvature of the wavefront, and ζ_j the Gouy phase of the jth filament. The width w_j is defined as the radius at which the field amplitude drops to $1/e^2$ of its maximum value and $w_{0,j}$ is the minimal width of the jth mode at the beam waist, located at $z = 0$.

The propagation of the field $E_j(x, z)$ of each filament for a distance z is described as follows:

$$w_j(z) = w_{0,j}\sqrt{1 + \left(\frac{z}{z_{r,j}}\right)^2} \tag{2}$$

$$R_j(z) = z\left[1 + \left(\frac{z_{r,j}}{z}\right)^2\right] \tag{3}$$

$$\zeta_j(z) = \arctan\left(\frac{z}{z_{r,j}}\right) \tag{4}$$

where

$$z_{r,j} = \frac{\pi w_{0,j}^2}{\lambda} \tag{5}$$

is the Rayleigh range.

The intensity $\mathcal{I}$ of the optical mode at any point during the propagation from the near-field to the far-field is then given by

$$\mathcal{I}(x, z) = \left|\sum_{j=1}^{N} E_j(x, z)\right|^2. \tag{6}$$

In the first step of the phase reconstruction procedure we fit the lateral near-field profile $\mathcal{I}(x, z = 0)$. The corresponding fitting parameters are amplitude A_j, width w_j, and lateral position ξ_j of the single filaments at $z = 0$. The relative phase ϕ_j of the different modes is initially set to zero.

In the next step the lateral intensity profile $\mathcal{I}(x, z_1)$ in a certain distance z_1 is calculated and fitted to the corresponding measurement at position z_1, where now the phase constants ϕ_j are the fitting parameters and all other parameters are kept constant. Then again the near-field profile $\mathcal{I}(x, z = 0)$ is fitted, but now with phase constants ϕ_j from the fit at $z = z_1$ and so on. In most cases after a few iterations a good fitting result is obtained. This procedure is similar to the Gerchberg–Saxton algorithm [20], but we use only N discrete values to fit the phase distribution. In the physical context of coupled filaments this approach provides enough degrees of freedom to describe the near-field to far-field evolution.

We apply this fitting routine with $N = 4$ filaments to the bottom and top lines of the measurement shown in Fig. 4(a), representing the lateral near-field profile at $z = 0$ and the propagated mode profile at $z_1 = 200$ μm, respectively. From this simultaneous fit to the measured intensity profiles for $z = 0$ and $z = z_1$ we know now the field and the phase distribution of the laser mode at the output facet and thus we can reconstruct the complete propagation of the lateral mode profile from the near-field into the far-field. Fig. 4(b) shows the result of the reconstructed propagation for $0 < z < z_1$ and the result is in excellent agreement with the corresponding measurement, shown in Fig. 4(a).

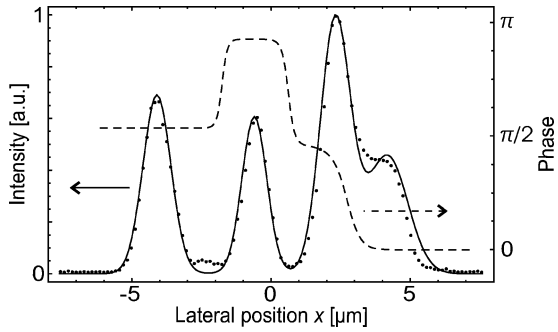

Fig. 5. Lateral near-field intensity and phase profile of sample B at $\mathcal{I} = 1.23I_{\mathrm{th}}$. The dots represent the experimental data, solid and dashed lines show the result of the fitting procedure for the lateral intensity profile and the corresponding phase distribution, respectively.

The result of the near-field phase reconstruction is plotted as dashed line in Fig. 5, together with the corresponding fit of the near-field intensity profile (solid line) to the experimental data (dots). Obviously there is a phase offset $\Delta\phi$ of about $\pm\pi/2$ between adjacent filaments. This observation is in agreement with simulations by Chow *et al.* [8]. They calculated the lateral near-field distribution for a gain-guided edge-emitting LD with 6 μm stripe width and 2 nm $In_{0.2}Ga_{0.8}N/GaN$ multiple quantum well structure. The results show also a phase difference $0 < \Delta\phi < \pi$ between two filaments, which have a FWHM of about 1.9μm each.

In the following this result will be compared to observations on LDs in the GaAs material system: In [12] and [18] arrays of phase-locked filaments in broad ridge GaAs LDs are observed, which produce a single lobed lateral far-field intensity distribution. This indicates, that all filaments lock in phase ($\Delta\phi = 0$), which the authors attribute to the fact that in a self focused multifilamentary laser there is high gain in the regions of low refractive index and vice versa. Logically consistent, Ackley *et al.* observe a lateral far-field pattern with a symmetric double-peak for an array of coupled LDs [23]. Their structure provides gain only in the regions of high refractive index, where the single LDs are located. Thus adjacent emitters couple out of phase ($\Delta\phi = \pi$), to minimize the optical field in the unpumped or absorbing interstripe regions and maximize the overlap of the optical field with the lateral spatial gain distribution. Kish *et al.* managed stable in-phase operation of neighboring emitters in an array of LDs by a precise adjustment of the lateral optical and current confinement [24].

Summarized, in the GaAs material system there seems to exist a consistent model, which describes the coupling mechanism between phase-locked filaments in broad area LDs or between single emitters in LD arrays. But coupled filaments in (Al,In)GaN LDs seem to behave differently, although the configuration in the waveguide should be comparable to the situation described in [12] and [18] for filaments in GaAs LDs. Due to spatial hole burning, filamentation provides a higher carrier density and thus higher gain in the regions between the filaments. This constellation is expected to lead to an in-phase coupling of the filaments, in order to maximize the overlap of the

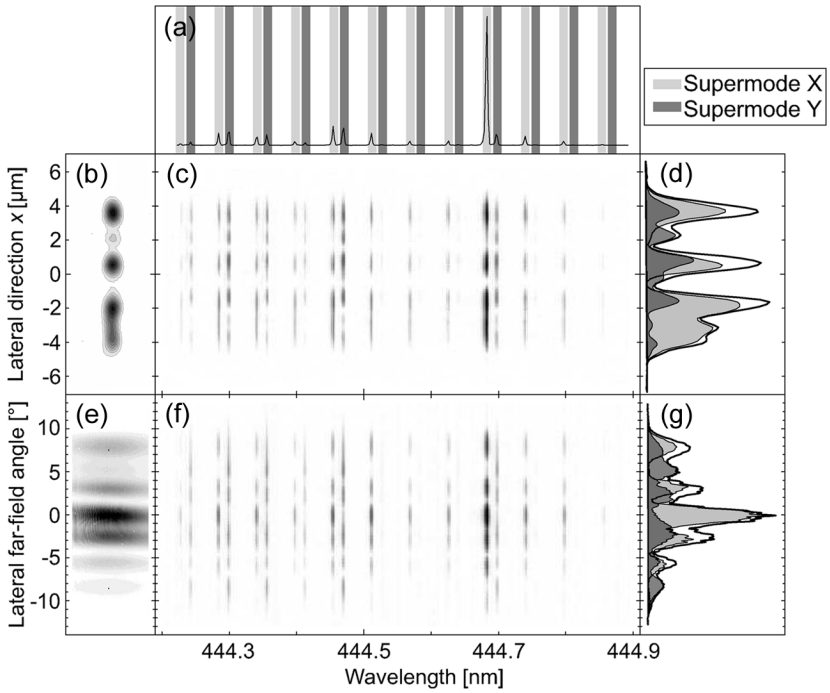

Fig. 6. (a) Spatially integrated spectrum of sample B at $I = 1.54I_{\rm th}$. (b), (e) Images of the near-field and far-field intensity distribution, respectively. (c), (f) Corresponding spatially resolved spectral characterization of the lateral mode profile. (d), (g) Lateral intensity profile (black line) in the near-field and in the far-field, respectively. The laser mode is a superposition of two supermodes X (light gray filling) and Y (dark gray filling), marked by light gray and dark gray bars in (a).

lateral optical field with the lateral gain profile. But we did neither observe strict in-phase coupling nor strict out-of-phase coupling of neighboring filaments at any broad ridge (Al,In)GaN LD. The reconstructed phase distributions of different supermodes look qualitatively similar to the one shown in Fig. 5 for sample B. In general a phase difference $0 < \Delta\phi < \pi$ between adjacent filaments is observed. Up to now we found no satisfying explanation for this behavior. Due to material inhomogeneities the single filaments have different intensities, which leads to an inhomogeneous and asymmetric gain and refractive index profile across the waveguide. Maximization of the overlap of the lateral optical field in this modified refractive index profile with the lateral gain profile may lead to the observed behavior. Further investigations, experimentally and theoretically, will be necessary to completely understand the observed behavior.

IV. Incoherent Superposition of Supermodes

All measurements shown in Section III were taken at about $I = 1.2I_{\rm th}$ to stay in the regime of phase-locked filaments, but the investigated broad ridge laser diodes are designed for high output power at much higher driving currents. But with increasing current the laser spectrum becomes more complex and coexistence of different supermodes, leading to modifications of the lateral near-field and far-field profile, is observed. This behavior will be discussed in the following section.

A. Two Supermodes

In the spatially integrated spectrum of sample B at a current of $I = 1.54I_{\rm th}$, shown in Fig. 6(a), clearly two FP mode combs can be observed. This indicates the coexistence of one or more new filaments building an additional supermode with a different effective refractive index $n_{\rm eff}$ and thus different propagation constant.

To separate the lateral profile of the two supermodes with different propagation constants, we combine again spatial and spectral information. The corresponding data for the near-field case are shown in Fig. 6(b)–(d). Fig. 6(c) shows a spectrally resolved lateral scan through the near-field laser mode, which is depicted in Fig. 6(b). Obviously the two FP mode combs, named X and Y and marked by light gray and dark gray bars in Fig. 6(a), respectively, show a completely different lateral behavior. So for example at about $x = 2.5$ μm only the supermode Y is lasing, and for $x < -3$ μm the supermode Y dominates. By integrating over the light and dark gray regions marked in Fig. 6(a) we can present the spectrally integrated lateral profile (black line in Fig. 6(d)) as incoherent superposition of the two supermodes X and Y (light and dark gray filling, respectively). The analogue data for the far-field case are shown in Fig. 6(e)–(g). Also here the two supermodes can be clearly separated.

The two supermodes have different FP mode combs, thus they are not phase-locked and propagate independently. Hence we perform the fitting procedure described in Section III-D for the two supermodes separately. Fig. 7(a) and (b) show the simulated propagation of supermode X and Y for 0 μm $< z <$ 200 μm, respectively. The gray-scale is separately normalized for part (a) and (b) with respect to the different relative intensities of the two supermodes.

The correctness of this reconstructed propagation can not be proven directly by comparison with experimental data. A direct measurement of the propagation of the different supermodes

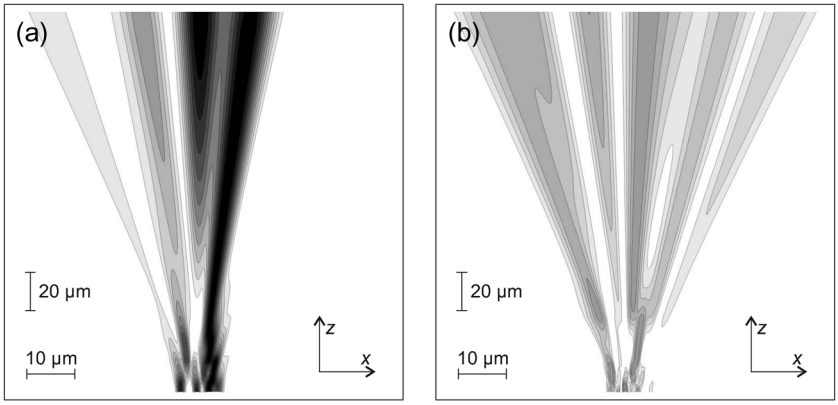

Fig. 7. Reconstructed propagation of the lateral intensity profile of (a) supermode X and (b) supermode Y of sample B at $I = 1.54I_{\mathrm{th}}$. The experimental data for the fits are the near-field and far-field mode profiles of the two supermodes shown in Fig. 6(d) and (g), respectively.

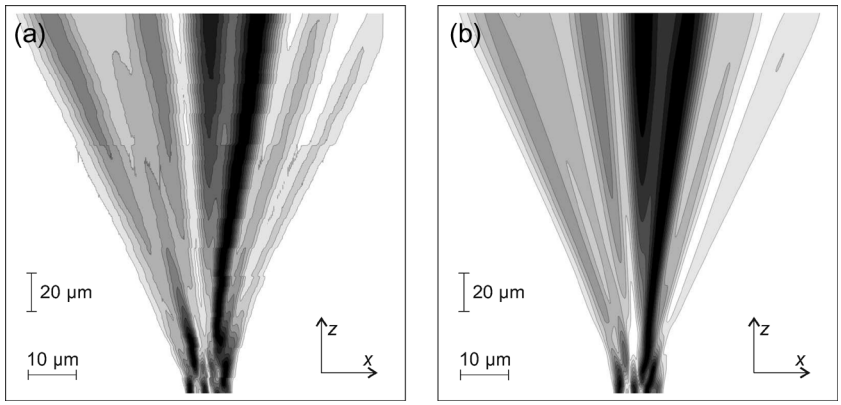

Fig. 8. (a) Measured propagation of the lateral intensity profile of sample B at $I = 1.54I_{\mathrm{th}}$. (b) Incoherent superposition of the reconstructed propagation of supermodes X and Y, shown in Fig. 7(a) and (b), respectively.

would be too extensive, because a full spectrum would have to be measured at each point (x, z) of the scan.

But it is possible to measure the propagation of the spectral integrated intensity profile, which is shown in Fig. 8(a), because this can be done simply in the same way as for the single supermode case shown in Fig. 4(a). This measurement can be compared to the sum of the intensities of the simulated propagation of the two supermodes X and Y with respect to their relative intensities. The result of this incoherent superposition of the two supermodes, depicted in Fig. 8(b), is again in very good agreement with the experimentally observed propagation pattern for this driving current.

An interesting point is, that the propagation of supermode X at $I = 1.54I_{\mathrm{th}}$, shown in Fig. 7(a), is very similar to the single supermode case described in Fig. 4. This means, that this supermode seems to be hardly influenced by the second supermode Y, although they are spatially and spectrally overlapping. We do not observe a pronounced coherent coupling of lateral modes with different propagation constants like it is described for example in [25] for different lateral modes in a GaAs LD.

B. Multiple Supermodes

The situation becomes even more complex at higher driving currents. Due to the deposited heat by injected power the waveguide temperature increases with increasing current. In [26] we have shown that in pulsed operation a critical wave-guide temperature for the build-up of certain filaments exists. Temperature changes modify the refractive index profile of the LD waveguide as well as the bandgap energy and thus the peak gain wavelength. This leads to appearance, disappearance and modifications of single supermodes depending on driving current and temperature.

In general, at higher driving currents several supermodes coexist. Fig. 9 shows the lateral near-field (a) and far-field (b) profile of sample B at $I = 3.1I_{\mathrm{th}}$. From spatially and spectrally resolved measurements, similar to those shown in Fig. 6 for $I = 1.54I_{\mathrm{th}}$, we can in this case separate the lateral intensity profile (thick line in Fig. 9) into five supermodes, that are plotted as thin lines. Supermodes X and Y from Fig. 6 are still existing at this high driving current and they look quite similar to the lower driving current case as well in the near-field as in the far-field. For clarity only supermode X is marked by a light gray filling in Fig. 9.

The lateral near-field intensity profile at $I = 3.1I_{\mathrm{th}}$ looks much more uniformly than at $I = 1.2I_{\mathrm{th}}$, which is shown in Fig. 3(b). Thus it seems like the different supermodes tend to fill up the waveguide. And as different supermodes show completely different propagation patterns, also the lateral far-field pattern becomes smoother by this incoherent superposition of the multi-lobed far-field patterns of the single supermodes

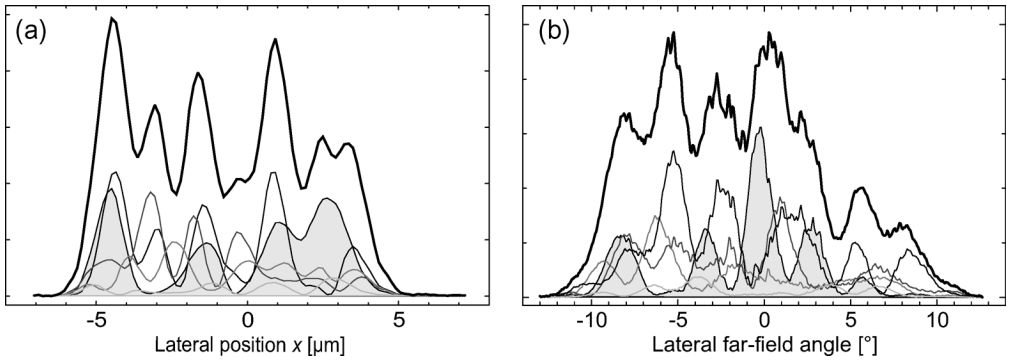

Fig. 9. Lateral near-field (a) and far-field (b) profile of sample B at $I = 3.1I_{\mathrm{th}}$. Five supermodes (thin lines) coexist and add up to the lateral intensity profile (thick line).

[compare thick lines in Fig. 9(b) and Fig. 9(d)]. Thus the absence of distinct filaments in the near-field or the lack of pronounced lobes in the lateral far-field pattern does not imply the absence of supermodes, but this observation may be due to an incoherent superposition of several supermodes.

Another relevant point is that the $I - P$ characteristic of sample B shows a kink at about $I_{\mathrm{kink}} = 1.3I_{\mathrm{th}}$. The slope efficiency is slightly increased for $I > I_{\mathrm{kink}}$. Interestingly, I_{kink} marks the transition from the single supermode to the multiple supermode configuration. Thus it seems that the incoherent superposition of supermodes associated with the filling of the waveguide improves the efficiency of the LD.

V. Conclusion

We have shown that the laser mode of broad ridge (Al,In)GaN based LDs consists of phase-locked filaments forming so called supermodes. This means that the far-field of these diodes is defined by interference effects and shows a characteristic multi-lobed pattern. Depending on driving current, one or more of these supermodes exist, which can be identified by their spectral composition. Different supermodes propagate independently and thus the resulting laser beam is an incoherent superposition of these supermodes. In this way the far-field pattern of these broad ridge LDs depends significantly on driving current. For high driving current several supermodes coexist, which tend to fill up the waveguide.

We are able to reconstruct the propagation of these supermodes by a superposition of Gaussian beams, which represent the filaments. In this way we determine the phase distribution of the laser mode, which provides essential information about the coupling of the filaments. We do observe neither an in-phase nor a strict out-of-phase coupling between neighboring filaments, which seems to be different to other material systems.

We would like to point out, that the existence of supermodes was observed at all investigated broad ridge (Al,In)GaN LDs independent on emission wavelength or modifications of the epitaxial structure, whereas the exact shape of the supermodes is individual but characteristic and reproducible for each sample. Also experimental far-field data provided by other groups [3] exhibit the features of phase-locked filaments, which indicates that the existence of supermodes is a basic feature of broad ridge (Al,In)GaN LDs.

An important question is of course, how the beam quality of high power (Al,In)GaN LDs could be improved. We think that filamentation itself cannot be suppressed in broad ridge (Al,In)GaN LDs, but it may be possible to control and direct the filamentation by a lateral periodic perturbation of the broad area laser structure, as it is for example realized for a broad area LD in the GaAs material system by a lateral modulation of the mirror reflectivity [12]. In principle, there are two different ways of perturbation, either the real part or the imaginary part of the refractive index profile can be modulated, resulting in index-guided or gain-guided structures, respectively. This approach is of course very close to the idea of laser diode arrays, which have already been realized in the (Al,In)GaN material system [3], [27]. However, stable in-phase coupling of the single emitters or filaments over a wide current range has to be achieved, to produce a stable laser beam for high power applications.

References

[1] U. Strauß, S. Brüninghoff, M. Schillgalies, C. Vierheilig, N. Gmeinwieser, V. Kümmler, G. Brüderl, S. Lutgen, A. Avramescu, D. Queren, D. Dini, C. Eichler, A. Lell, and U. T. Schwarz, "True-blue InGaN laser for pico size projectors," *Proc. SPIE*, vol. 6894, no. 1, p. 689417 [Online]. Available: http://link.aip.org/link/?PSI/6894/689417/1

[2] S. Brüninghoff, S. Eichler, S. Tautz, A. Lell, M. Sabathil, S. Lutgen, and U. Strauß, "8 W single-emitter InGaN laser in pulsed operation," *Phys. Status Solidi (A),* vol. 206, no. 6, pp. 1149–1152, 2009 [Online]. Available: http://dx.doi.org/10.1002/pssa.200880859

[3] S. Goto, M. Ohta, Y. Yabuki, Y. Hoshina, K. Naganuma, K. Tamamura, T. Hashizu, and M. Ikeda, "Super high-power AlGaInN-based laser diodes with a single broad-area stripe emitter fabricated on a GaN substrate," *Phys. Status Solidi (A),* vol. 200, no. 1, p. 122, 2003 [Online]. Available: http://dx.doi.org/10.1002/pssa.200303325

[4] T. Swietlik, G. Franssen, R. Czernecki, M. Leszczynski, C. Skierbiszewski, I. Grzegory, T. Suski, P. Perlin, C. Lauterbach, and U. T. Schwarz, "Mode dynamics of high power (InAl)GaN based laser diodes grown on bulk GaN substrate," *J. Appl. Phys.,* vol. 101, no. 8, p. 083109, 2007 [Online]. Available: http://link.aip.org/link/?JAP/101/083109/1

[5] M. Ohta, Y. Ohizumi, Y. Hoshina, T. Tanaka, Y. Yabuki, K. Funato, S. Tomiya, S. Goto, and M. Ikeda, "High-power pure blue laser diodes," *Phys. Status Solidi (A),* vol. 204, p. 2068, 2007 [Online]. Available: http://dx.doi.org/10.1002/pssa.200674748

[6] C. Eichler, D. Hofstetter, W. W. Chow, S. Miller, A. Weimar, A. Lell, and V. Härle, "Microsecond time scale lateral-mode dynamics in a narrow stripe InGaN laser," *Appl. Phys. Lett.,* vol. 84, no. 14, pp. 2473–2475, 2004 [Online]. Available: http://link.aip.org/link/?APL/84/2473/1

[7] U. T. Schwarz, E. Sturm, W. Wegscheider, V. Kümmler, A. Lell, and V. Härle, "Optical gain, carrier-induced phase shift, and linewidth enhancement factor in InGaN quantum well lasers," *Appl. Phys. Lett.,* vol. 83, no. 20, pp. 4095–4097, 2003 [Online]. Available: http://link.aip.org/link/?APL/83/4095/1

[8] W. W. Chow, H. Amano, and I. Akasaki, "Theoretical analysis of filamentation and fundamental-mode operation in InGaN quantum well lasers," *Appl. Phys. Lett.,* vol. 76, no. 13, pp. 1647–1649, 2000 [Online]. Available: http://link.aip.org/link/?APL/76/1647/1

[9] W. W. Chow and H. Amano, "Analysis of lateral-mode behavior in broad-area InGaN quantum-well lasers," *IEEE J. Quantum Electron.*, vol. 37, pp. 265–273, 2001.

[10] M. Pindl and U. T. Schwarz, "Waveguide mode dynamics of blue laser diodes," *Phys. Status Solidi (A),* vol. 203, p. 1787, 2006 [Online]. Available: http://dx.doi.org/10.1002/pssa.200565248

[11] H. Braun, H.-M. Solowan, D. Scholz, T. Meyer, U. T. Schwarz, S. Brüninghoff, A. Lell, and U. Strauß, "Lateral and longitudinal mode pattern of broad ridge 405 nm (Al,In)GaN laser diodes," *J. Appl. Phys.,* vol. 103, no. 7, p. 073102, 2008 [Online]. Available: http://link.aip.org/link/?JAP/103/073102/1

[12] J. Salzman, A. Larsson, and A. Yariv, "Phase-locked controlled filament laser," *Appl. Phys. Lett.,* vol. 49, no. 11, pp. 611–613, 1986 [Online]. Available: http://link.aip.org/link/?APL/49/611/1

[13] J. Buus, "Models of the static and dynamic behavior of stripe geometry lasers," *IEEE J. Quantum Electron.*, vol. QE-19, no. 6, pp. 953–960, Jun. 1983.

[14] D. Y. Li, Y. Z. Huang, J. J. Zhu, D. G. Zhao, Z. S. Liu, S. M. Zhang, X. J. Ye, M. Chong, L. H. Chen, H. Yang, and J. W. Liang, "Thermal lensing effect in ridge structure InGaN multiple quantum well laser diodes," *J. Appl. Phys.,* vol. 100, no. 4, p. 046101, 2006 [Online]. Available: http://link.aip.org/link/?JAP/100/046101/1

[15] D. Scholz, H. Braun, U. T. Schwarz, S. Brüninghoff, D. Queren, A. Lell, and U. Strauss, "Measurement and simulation of filamentation in (Al,In)GaN laser diodes," *Opt. Expr.,* vol. 16, no. 10, pp. 6846–6859, 2008 [Online]. Available: http://www.opticsexpress.org/abstract.cfm?URI=oe-16-10-6846

[16] S. Rogowsky, H. Braun, U. T. Schwarz, S. Brüninghoff, A. Lell, and U. Strauü, "Multidimensional near- and far-field characterization of broad ridge (Al,In)GaN laser diodes," *Phys. Status Solidi (C),* 2009 [Online]. Available: http://dx.doi.org/10.1002/pssc.200880853

[17] E. Kapon, Z. Rav-Noy, L. T. Lu, M. Yi, S. Margalit, and A. Yariv, "Phase-locking characteristics of coupled ridge-waveguide InP/InGaAsP diode lasers," *Appl. Phys. Lett.,* vol. 45, no. 11, pp. 1159–1161, 1984 [Online]. Available: http://link.aip.org/link/?APL/45/1159/1

[18] A. Larsson, J. Salzman, M. Mittelstein, and A. Yariv, "Lateral coherence properties of broad-area semiconductor quantum well lasers," *J. Appl. Phys.,* vol. 60, no. 1, pp. 66–68, 1986 [Online]. Available: http://link.aip.org/link/?JAP/60/66/1

[19] A. Moritz, R. Wirth, C. Geng, F. Scholz, and A. Hangleiter, "Birefringence and tilted modes in ordered GaInP/AlGaInP waveguides and lasers," *Appl. Phys. Lett.,* vol. 68, no. 9, pp. 1217–1219, 1996 [Online]. Available: http://link.aip.org/link/?APL/68/1217/1

[20] R. W. Gerchberg and W. O. Saxton, "A practical algorithm for the determination of phase from image and diffraction plane pictures," *Optik*, vol. 35, p. 227, 1972.

[21] U. T. Schwarz, M. Pindl, W. Wegscheider, C. Eichler, F. Scholz, M. Furitsch, A. Leber, S. Miller, A. Lell, and V. Hürle, "Near-field and far-field dynamics of (Al,In)GaN laser diodes," *Appl. Phys. Lett.,* vol. 86, no. 16, p. 161112, 2005 [Online]. Available: http://link.aip.org/link/?APL/86/161112/1

[22] A. E. Siegman*, Lasers*. Mill Valley, CA: University Science Books, 1986.

[23] D. E. Ackley, "Single longitudinal mode operation of high power multiple-stripe injection lasers," *Appl. Phys. Lett.,* vol. 42, no. 2, pp. 152–154, 1983 [Online]. Available: http://link.aip.org/link/?APL/42/152/1

[24] F. A. Kish, S. J. Caracci, J. N. Holonyak, P. Gavrilovic, K. Meehan, and J. E. Williams, "Coupled-stripe in-phase operation of planar native-oxide index-guided $Al_yGa_{1-y}As$-GaAs-$In_xGa_{1-x}As$ quantum-well heterostructure laser arrays," *Appl. Phys. Lett.,* vol. 60, no. 1, pp. 71–73, 1992 [Online]. Available: http://link.aip.org/link/?APL/60/71/1

[25] W. D. Herzog, B. B. Goldberg, and M. S. Unlu, "Beam steering in narrow-stripe high-power 980-nm laser diodes," *IEEE Photon. Technol. Lett.* vol. 12, no. 12, pp. 1604–1606, Dec. 2000.

[26] H. Braun, D. Scholz, T. Meyer, U. T. Schwarz, D. Queren, M. Schillgalies, S. Brüninghoff, A. Laubsch, and U. Strauss, "Measurement and simulation of the lateral mode profile of broad ridge 405 nm (Al,In)GaN laser diodes," *Proc. SPIE*, vol. 6997, no. 1, p. 69971U [Online]. Available: http://link.aip.org/link/?PSI/6997/69971U/1

[27] K. Holc, P. Wisniewski, M. Leszczynski, T. Suski, I. Grzegory, R. Czernecki, S. Grzanka, and P. Perlin, "Violet blue laser mini-bars," *Phys. Status Solidi (C)*, vol. 6, no. S2, pp. S837–S839, 2009.

Harald Braun received the Diploma in experimental physics in 2005 from the University of Regensburg, Germany. Since 2005 he has been working towards the Ph.D. degree at the University of Regensburg, Germany. His research is in the field of optical characterization of nitride based semiconductor lasers.

Stephan Rogowsky received the Diploma from the University of Regensburg, Germany, in 2008 and is currently pursuing the Ph.D. degree at the Fraunhofer Institute for Applied Solid State Physics IAF, Freiburg, Germany.

His scientific interests lie in the development of monolithically integrated laser structures on silicon substrate.

Ulrich T. Schwarz received the Ph.D. degree in physical science in 1997 from the University of Regensburg, Germany.

In 2004, he concluded his habilitation and since then has been with the faculty as an Assistant Professor. His research is in the field of optical characterization of nitride semiconductors and laser dynamics. Another focus is on singular optics, in particular polarization singularities. Awarded by the Alexander von Humboldt foundation with a Feodor Lynen scholarship, he spent two postdoctorial years (1997–1999) at Cornell University, Ithaca, NY, with research on intrinsically localized modes. In 2001 he joined the group of Prof. R. Grober at Yale University, New Haven, CT. In 2006/2007, he visited Kyoto University, Kyoto, Japan, with an invited fellowship (long-term) awarded by the Japanese Society for the Promotion of Science.

Dr. Schwarz is a member of the Optical Society of America (OSA), American Physical Society (APS), International Society for Optical Engineering (SPIE), and the German Physical Society (DPG).

Stefanie Brüninghoff received the Dipl.-Ing. degree in electrical engineering and information technology from the RWTH Aachen University, Aachen, Germany, in 2006. Since 2006 she has been working towards the Ph.D. degree at OSRAM Opto Semiconductors GmbH, Regensburg, Germany, on the field chip technology of InGaN lasers. The main topic of her work is the development of InGaN-based high-power lasers.

Alfred Lell received the Diploma in experimental physics from the University of Regensburg, Germany, in 1986. Then he joined the Research and Development Department at Siemens Semiconductor group, Regensburg, Germany, working on the development of LEDs, Hall sensors and detector arrays. In 1992 he joined the laser group and took over the responsibility of the telecommunication laser research and development activities of Siemens Regensburg. Since 1998 he has been working on InGaN based laser diodes, and since 2001 he has been Project Leader of Blue Laser Diodes at OSRAM Opto Semiconductors GmbH, Regensburg, Germany.

Stephan Lutgen received the Diploma in physics from the University of Marburg in 1993. His dissertation at the Max-Born-Institut at Berlin was on femtosecond infrared spectroscopy of the coherent and incoherent intersubband dynamics in GaInAs/AlInAs quantum wells. He received the Ph.D. degree in physics from the Humbold University in Berlin in 1997.

He joined Siemens in 1997 as MOVPE production engineer for InGaAs-AlGaAs based LEDs, high power lasers and VCSELs. In 2000 he was engaged in the R&D group as project leader for frequency doubled blue and green GaAs-based VECSELs for RGB-laser projection. In 2005 he was project leader of blue InGaN-Laser at Osram. Today he is Head of InGaN-Laser R&D at OSRAM Opto Semiconductors GmbH.

Uwe Strauß received the Diploma in physics at the University of Braunschweig, Germany, in 1991. From 1991 to 1993 he focused on opto-semiconductor basic research at the Max-Planck-Institute for Solid State Research. In 1994 he received the Ph.D. degree at the University of Stuttgart. Then he joined semiconductor industry. His research interests are novel optoelectronical devices. Today he is heading the semiconductor laser development at OSRAM Opto Semiconductors GmbH.